0026-895X/89/020223-09$02.00/0

MOLECULAR PHARMACOLOGY, 35:223-231

N-Methylanatoxinol Isomers: Derivatives of the Agonist (+)-Anatoxin-a Block the Nicotinic Acetylcholine Receptor Ion Channel

K. L. SWANSON, Y. ARACAVA, F. J. SARDINA, H. RAPOPORT, R. S. ARONSTAM, and E. X. ALBUQUERQUE

Department of Pharmacology and Experimental Therapeutics, University of Maryland School of Medicine, Baltimore, Maryland 21201 (K.L.S., Y.A., E.X.A.), Laboratory of Molecular Pharmacology II, Institute of Biophysics "Carlos Chagas Filho," Federal University of Rio de Janeiro, Ilha do Fundão, CEP 21941, RJ, Brazil (Y.A., E.X.A.), Department of Chemistry, University of California, Berkeley, California 94720 (F.J.S., H.R.), and Department of Pharmacology and Toxicology, Medical College of Georgia, Augusta, Georgia 30912 (R.S.A.)

Received April 4, 1988; Accepted November 10, 1988

SUMMARY

Using biochemical and patch-clamp techniques, we investigated the pharmacology of *S*- and *R*-epimers of *N*-methylanatoxinol, which are analogs of the semi-rigid, stereoselective, nicotinic agonist (+)-anatoxin-a. In contrast to (+)-anatoxin-a, both isomers had poor ability to inhibit the binding of ^{125}I-α-bungarotoxin or to open acetylcholine channels, and they were unable to elicit contracture of frog rectus abdominis muscles. However, both isomers were able to demonstrate significant concentration-dependent blockade of the nicotinic acetylcholine receptor ion channel. The *R*-isomer was approximately 4-fold more potent in causing inhibition of [^{3}H]H_{12}HTX binding than was the *S*-isomer, in the absence of carbamylcholine. In the presence of carbamylcholine, the affinity of the *R*-isomer of *N*-methylanatoxinol for the ion channel sites was further enhanced, so that its affinity became much greater than that of the *S*-isomer. Refinement of voltage- and concentration-dependent terms for the ion channel blocking and unblocking rates yielded functions that were able to predict the channel open times and short closed times well. The *S*-isomer bound and dissociated from the ion channel site of the nicotinic acetylcholine receptor more rapidly and with greater voltage sensitivity than the *R*-isomer. The present characterization of the antagonistic properties of these new analogs of (+)-anatoxin-a introduces a new aspect to the molecular pharmacology of (+)-anatoxin-a analogs; the semi-rigid compounds could be useful in describing the allosteric binding sites of the acetylcholine receptor, as well as in delimiting the agonist binding site.

The opportunity to examine the structural specificity of nicotinic receptors has been expanded by the use of semi-rigid ligands that have agonistic effects (1–3). Previously, the chemical characterization of agonists suitable for the activation of the nicotinic AChR was based on correlations among several flexible structures; these structures were proposed to assume conformations with similar cation (alkyl ammonium) to carbonyl separations and orientations (4) and to have a planar region for hydrogen bond formation (5). Studies that characterized the topology and chemistry of the receptor binding sites often utilized antagonists (6, 7) or they characterized the desensitized or chemically reduced forms of the receptor (8, 9).

The natural toxin found in the blue green algae *Anabaena flos-aquae* (1, 10) not only is semi-rigid but also has marked stereospecificity (11) for the peripheral nicotine AChR. The nicotinic AChR of the CNS has been difficult to study. Because (+)-anatoxin-a is a secondary amine but not an ester (and is therefore resistant to enzymatic hydrolysis) and because it is 100-fold more selective for nicotinic receptors than for muscarinic receptors (12), the toxin has become a very useful agent for investigation of the nicotinic receptor of the CNS (13–15, 19). Its potential regarding CNS diseases in which nicotinic transmission is pathologically altered (16–18) remains to be explored.

At the peripheral nicotinic receptor, the natural isomer, (+)-anatoxin-a, is a much more potent agonist than carbamylcholine, because of the greater binding affinity of the toxin for the ACh site (11). The synthetic enantiomer, (−)-anatoxin-a, has low affinity for the receptor and, therefore, low potency as a nicotinic agonist. Another feature of (+)-anatoxin-a is its selectivity primarily for agonistic effects and secondarily for

F.J.S. thanks the Spanish Ministry of Education and Science and the Fulbright Commission for a fellowship. K.L.S. thanks the National Biomedical Simulation Resource, Duke University, Durham NC, for training in the use of the Simulation Control Program (SCoP) supported by National Institutes of Health Grant RR01693. This work was supported by National Institutes of Health Grants NS25296 and GM37948.

ABBREVIATIONS: AChR, acetylcholine receptor; ion channel; CNS, central nervous system; ACh, acetylcholine; α-BGT, α-bungarotoxin; H_{12}-HTX, perhydroistrionicotoxin; HEPES, 4-(2-hydroxyethyl)-1-piperazineethanesulfonic acid; CBZ, benzyloxycarbonyl; 2D, two-dimensional.

desensitizing effects (19), whereas other nicotinic agonists demonstrate ion channel-blocking actions at concentrations closer to their agonistic concentrations (20, 21). Unfortunately, for many agonists complete pharmacological studies have not been done to distinguish combined agonist-antagonist properties from low agonist potency.

In the present study, the *S*- and *R*-geometric isomers of *N*-methylanatoxinol (Fig. 1) were investigated for potency as agonists and as antagonists. The low contracture potency for these analogs is related to a low affinity for the α-BGT binding site of the receptor and to a low stimulation of channel activity. Further characterization of the new compounds with regard to their ability to inhibit twitch, to interact with H_{12}-HTX binding sites, and to block ion channels introduces a new aspect to the molecular pharmacology of (+)-anatoxin-a analogs; these semi-rigid compounds could be as useful in describing the allosteric binding sites of the AChR as they are in delimiting the agonist binding site.

Materials and Methods

Solutions and drugs. Ringer's solutions consisted of (mM): NaCl, 116; KCl, 2; $CaCl_2$, 1.8; Na_2HPO_4, 1.3; and NaH_2PO_4, 0.7. HEPES-buffered solution consisted of (mM): NaCl, 115; KCl, 2.5; $CaCl_2$, 1.8; and HEPES, 3, adjusted to pH 7.1 with NaOH. The synthesis of (+)-anatoxin-a HCl was described previously (22) and the synthesis of the *N*-methylanatoxinols is described below. All drug solutions were stored frozen.

Synthesis of *N*-methylanatoxinols [(1*R*,10*R*)- and (1*R*,10*S*)-2(10-hydroxyethyl)-9-methyl-9-azabicyclo[4.2.1]-2-nonene]. The synthesis (Fig. 1) of the *N*-methylanatoxinols **g** and **h** was accomplished as follows: CBZ-dihydroanatoxin, **c**, obtained from (+)-dihydroanatoxin, **b** (22), was converted to its trimethylsilyl enol ether, which was subsequently oxidized to give CBZ-anatoxin, **d**. Reduction of **d** with $NaBH_4/CeCl_3 \cdot H_2O$ afforded the CBZ-anatoxinols **e** and **f** as a 1:1 mixture. These isomers were separated and their stereochemistry was assigned by 2D-NMR techniques. Reduction of the individual isomers **e** and **f** with $LiAlH_4$ yielded the desired pure *N*-methylanatoxinols, **g** and **h**. With the amine protected, it was apparent that the CBZ-anatoxinols differed by 2-fold in their polarity (by thin layer chromatography) due to differences in the alcoholic portion of the molecule.

The relative stereochemistry of the carbinol carbons (C10) of the *N*-methylanatoxinols **g** and **h** was determined at the CBZ-anatoxinol **e**, **f** stage of the synthesis by use of high field 2D NMR spectroscopy. The 2D-nuclear Overhauser effect spectroscopy spectrum of the less polar diastereomer **f** (of the CBZ-anatoxinols **e** and **f**) revealed cross-peaks between H-3 and H-10 as well as between CH_3-11 and H-1, thus confirming the *R* configuration at C-10.

Compounds **g** and **h** will be referred to in this manuscript simply as (*S*)- and (*R*)-*N*-methylanatoxinol or *S*- and *R*-isomers, respectively. The (*S*)- and (*R*)-*N*-methylanatoxinols are stable compounds and were determined to be of >99.8% purity. The only possible contaminant, and that at less than 0.2%, could be the epimeric alcohol. (+)-Anatoxin-a cannot be present. *N*-Methylanatoxinols were recrystallized as the hydrogen fumarate salts (*S*, m.p. 130–131°; *R*, m.p. 191–192°). Anatoxin-a has a pK_a of 9.4 (22) and methylation of secondary amines does not alter the pK_a by more than a fraction of a pK unit (23). Both epimers have the same behavior on silica gel: the fumarate salts have R_F values of 0.32 in acetic acid/methanol, 1:9, and the free bases have R_F values of 0.11 in methanol. Thus, both epimers are quite polar.

Contracture and muscle twitch assays. The potency of the two analogs in inducing contracture of the rectus abdominis muscle from the frog *Rana pipiens* was compared with contractures induced by carbamylcholine and (+)-anatoxin-a. The ability of the analogs to inhibit indirect twitch was assayed using the frog sciatic nerve-sartorius muscle preparation. Force transducers, stimulators, and polygraph recordings were used as previously described (11). Due to the limited supply of analogs and the low or absent drug sensitivity at high micromolar concentrations, few muscles (three or four) were tested in each experiment.

Receptor binding assays. Membranes were prepared from the electric organs of *Torpedo californica* (Pacific Bio-Marine, Venice, CA) by homogenization in 20 volumes of 50 mM Tris·HCl, pH 7.4, containing 100 μM phenylmethylsulfonyl fluoride to prevent proteolysis. After filtration through gauze to remove undisrupted material, the suspension was centrifuged at 15,000 × *g* for 20 min, resuspended in fresh buffer, and used without further treatment.

The binding of the analogs to the nicotinic receptor of *Torpedo* was measured using ^{125}I-α-BGT exactly as has been previously described (11).

Toxin interactions with the high affinity, receptor-gated, ion channel site were measured using [^{3}H]H_{12}HTX (54.5 Ci/mmol) (24) as the probe. An aliquot of *Torpedo* membranes (25–50 μg of protein) was incubated with 2 nM [^{3}H]H_{12}HTX and a range of analog concentrations in 50 mM Tris·HCl, pH 7.4, for 45 min at room temperature. The suspension was then filtered through glass fiber filters (Whatman GF/B) that had been wetted with a 1% organosilane solution (Sigmacote; Sigma Chemical Co., St. Louis, MO) to eliminate [^{3}H]H_{12}HTX binding

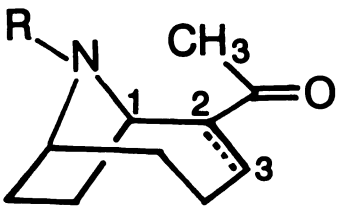

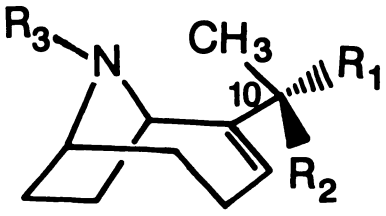

	R	C2–C3		R1	R2	R3	C10
a:	H	Δ	**e:**	OH	H	CBZ	S
b:	H		**f:**	H	OH	CBZ	R
c:	CBZ		**g:**	OH	H	CH_3	S
d:	CBZ	Δ	**h:**	H	OH	CH_3	R

Fig. 1. Synthesis of (*S*)- and (*R*)-*N*-methylanatoxinol. The analogs of the (+)-anatoxin-a (**a**) each differ from it by the addition of an *N*-methyl moiety and reduction of the carbonyl group, resulting in two stereospecific products. The synthesis (described more fully in the text) was from dihydroanatoxin (**b**) via formation of the CBZ derivatives and several steps of oxidation and reduction to produce the *N*-methylanatoxinols **g** and **h**, which are the *S*- and *R*-isomers, respectively. (The *symbol* Δ represents unsaturation on the C_2–C_3 bond.)

to the filters. The radioactivity content of the filters was determined by liquid scintillation counting. Nonspecific binding was measured in the presence of 100 μM amantadine (25). Ion channel binding was measured in the absence and presence of 1 μM carbamylcholine, because agonists enhance the binding affinity of most channel ligands (24, 26). K_i, inhibition constants, were determined from the IC_{50} values for inhibition of 2 nM [^{3}H]H_{12}HTX binding according to the relationship $K_i = IC_{50}/(1 + [D]/K_D)$, where $[D]$ and K_D are the [^{3}H]H_{12}HTX concentration and dissociation constant, respectively. The [^{3}H]H_{12}HTX dissociation constants were 0.089 and 0.135 μM in the presence and absence of 1 μM carbamylcholine, respectively.

Preparation of muscle fibers and patch clamp analysis. Single fibers were isolated from the interosseal muscle from the longest toe on the hind foot of the frog *R. pipiens* as originally described by Allen *et al.* (27). Briefly, treatment with collagenase (type I, Sigma; 1 mg/ml; 2 hr at 21°) followed by agitation in protease (type XXIV, Sigma; 0.2 mg/ml; 12 min) separated the muscle into individual fibers. Fibers were stored under refrigeration in HEPES buffer that contained bovine serum albumin (0.5 mg/ml). Tetrodotoxin (300 nM; Sankyo Labs) was added to HEPES-buffered solutions for all patch clamp studies in order to block Na^+ channel currents and to prevent contraction of the muscle fibers. All single channel recordings were performed at 10°.

Glass capillaries were pulled in two stages (Narishige PP-83) and fire-polished to yield patch electrodes with resistances of 4–8 MΩ. Gigaohm seals were formed with the perijunctional region of isolated muscle fibers using standard techniques. The LM-EPC-7 Patch Clamp System was used for voltage clamping. The signals were stored on FM magnetic tape for later analysis. The currents were low pass filtered at 3 KHz using an 8-pole Bessel filter before digitization at 80-μsec intervals, using IBM XT and AT microcomputers and PDP 11-24 and PDP 11-40 (Digital Equipment Corp., Marlboro, MA) minicomputers.

Analysis of amplitudes of single channel currents and lifetimes of open and closed states used the programs IPROC-2 and NFITS (M. Sloderbeck and C. J. Lingle, Florida State University) and programs using similar calculations, which have been previously described (11, 28). Transitions between open and closed states were identified by step changes of current that were greater than 50% of the mean channel current amplitude and more than 4 SD of the baseline noise; the thresholds for opening and closing were defined relative to the baseline current and the mean single channel current amplitude, respectively (see Ref. 29). Histograms of all closed event durations were composed of two exponentials. A closed interval longer than the majority of the short phase closed times (at least 4 times the mean duration of short closed times) was used as the criterion for burst discrimination. The durations of single openings, bursts, and short closed events were each fitted with single exponentials for determination of the time constants, τ. Because the long closed times between bursts were typically on the order of hundreds of milliseconds, they did not interfere with the exponential fitting of the short closed times, which were only a few milliseconds.

The sequential ion channel blocking model (30, 31) was used as a standard for comparison and description of molecular effects. In this model, the receptor (R) is bound by two molecules of ACh. The channel shifts to the open channel conformation, ACh_2R^*, and in the presence of blocking drug (D) leads to the formation of the drug-bound state ACh_2R^*D, which has no conductance. The predictions of the sequential model for open channel blockade include a linear concentration dependence according the relationship $1/\tau_{open} = k_{-2} + [D] \times k_3$ and a conservation of the total open time per burst. The data were quantified and evaluated to ascertain the appropriateness of this model for the effects produced by these toxin analogs.

Kinetic analysis in all cases was performed on the log(τ) because this

$$2\,ACh + R \underset{k_{-1}}{\overset{k_1}{\rightleftharpoons}} ACh_2R \underset{k_{-2}}{\overset{k_2}{\rightleftharpoons}} ACh_2R^* \underset{k_{-3}}{\overset{k_3}{\rightleftharpoons}} ACh_2R^*D \quad (k_3 = [D]\ k_{-3} = [D])$$

scale corrects the otherwise geometrically related confidence interval to have a constant relationship to the mean. Given that the 95% confidence interval for data along the line or curve is defined as $\log(\text{mean} \pm 1.96\ \sigma/\sqrt{n})$ and considering that the theoretical standard deviation (σ) of an exponential distribution is the same as its mean, the interval becomes $[\log(\text{mean}) + \log(1 + 1.96/\sqrt{n})]$ to $[\log(\text{mean}) + \log(1 - 1.96/\sqrt{n})]$, so that when n is constant the range on the log scale becomes constant. It is therefore unnecessary to use weighting factors in the regression analysis to correct for changes in σ that accompany changes in voltage. Weighting factors were not used to account for variations in n, as the standard errors were already quite small (see Fig. 5).

The voltage-dependent analysis was based on channel amplitude in pA, which is linearly related to voltage. The data for the log ($\tau_{open,\,control}$) versus channel amplitude were fitted by a linear regression to determine the duration and voltage-dependent coefficients for the channel closing rate, where $k_{-2} = B_{-2}e^{A_{-2}V}$ (32). Similarly, the data for the log ($\tau_{short\ closed}$) versus channel amplitude at all concentrations of drug were fitted by linear regression to determine the duration and voltage-dependent coefficients for the unblocking rate $k_{-3} = B_{-3}e^{A_{-3}V}$. For the drug blocking rate, data at multiple concentrations were modeled simultaneously by using the k_{-2} parameters just determined and estimates for the concentration- and time-dependent coefficient B_3 and voltage-dependent coefficient A_3 for the blocking rate constant $k_3 = B_3e^{A_3V}$ (33) in the equation $\tau_{open} = 1/(k_{-2} + k_3\,[\text{drug}])$. A parameter refinement procedure sought a minimum for the regression sum of squares difference $\sum (\log(\tau_{open,obs}) - \log(\tau_{open,calc}))^2$ using a simplex algorithm (34). The significance of the model was evaluated using a backwards elimination procedure (35). Simulation of the data was facilitated by the use of Simulation Control Program (SCoP version 2.6; National Biomedical Simulation Resource, Duke University, Durham, NC).

Results

Effects on muscle contracture and twitch. Neither the (S)- nor the (R)-*N*-methylanatoxinol isomers induced any detectible contracture of the rectus abdominis muscle at 0.012 to 170 μM and 0.12 to 250 μM, respectively. Because no hint of agonist efficacy was seen even at high concentrations, further contracture experiments were judged to be unnecessary.

Both analogs were subjected to preliminary testing for inhibition of receptor function using the indirect twitch assay. The strength of muscle twitch was apparently unaffected at all concentrations up to 400 μM of S-isomer (four muscles). The strength of muscle twitch decreased to 70% of control only when the highest concentration of the R-isomer (400 μM) was applied ($n = 2$).

Interactions with the ACh binding site of the AChR. Although ACh and (+)-anatoxin-a produced the expected inhibition of ^{125}I-α-BGT binding to *Torpedo* membranes, the analogs interacted poorly: the S-isomer inhibited ^{125}I-α-BGT slightly (10%) at 10 μM, but the inhibition due to the R-isomer was insignificant even at 100 μM.

Single channel activation. No significant agonist activity was demonstrated by contracture experiments for (S)- or (R)-*N*-methylanatoxinol. The possibility still existed that one could record a few single-channel events induced by these analogs, thus providing clues of the extent to which the structural modifications might influence the activation kinetics of AChR-ion channels, independent of effects on binding to the agonist site. In these experiments, ACh served as the control and did produce activation of channels in the endplate region of the isolated fibers, as previously disclosed (27).

Both *N*-methylanatoxinol analogs were then tested inde-

pendently on proven endplate regions for their ability to activate channels. The *R*-isomer was tested up to 200 μM, but no channels were activated. The (*S*)-*N*-methylanatoxinol did activate the channels of several patches when present in the micropipet at concentrations ≥ 1.25 μM (Fig. 2). These concentrations were much higher than those required for (+)-anatoxin-a, which activates single channel currents at 20 nM (11). The frequency of single channel activation induced by (*S*)-*N*-methylanatoxinol was also very low, with no multiple simultaneous openings, even when the analog concentrations were as high as 62.5–125 μM. For one patch, the channel activity observed at 1.25 μM (Fig. 2) consisted of openings of short duration (2.5 msec at 4.4 pA) and had "flickers" more frequently than ACh-induced channels but, due to their very low frequency, further kinetic evaluation was not done. A higher frequency of bursting was not observed at higher micromolar concentrations, and so it is possible that the patch recorded at 1.25 μM coincidentally had a large number of receptors. The channel activity observed at higher concentrations consisted of bursts of multiple repetitive openings, which appeared to be consistent with open channel-blocking activity. Even low concentrations of analogs in the presence of ACh were shown to produce channel blocking, described later in this paper, and very high micromolar concentrations of analogs were not considered to warrant further intensive investigation by the patch-clamp technique. Further analysis of these (*S*)-*N*-methylanatoxinol-induced channel events was not done and therefore no interpretation is available regarding the kinetics of receptor activation by the *S*-isomer.

Interaction with H_{12}-HTX binding sites. The inhibition of [^{3}H]H_{12}HTX binding by the analogs was assayed to detect interactions of the analogs with the receptor ion channel (Fig. 3). (*R*)-*N*-methylanatoxinol had 4 times greater potency for inhibiting [^{3}H]H_{12}HTX binding than did the *S*-isomer in the absence of carbamylcholine ($p < 0.01$; Table 1). Moreover, the affinity of the *R*-isomer was increased over 4-fold in the presence of carbamylcholine (1 μM). It should be noted that this change was independent of carbamylcholine effects on [^{3}H]H_{12}HTX binding itself. In contrast, the affinity of (*S*)-*N*-methylanatoxinol was not significantly affected by carbamylcholine (Fig. 3; Table 1).

Ion channel blocking by anatoxin analogs. Nicotinic ion channel activity was recorded directly using admixtures of ACh (0.4 μM) with (*S*)- or (*R*)-*N*-methylanatoxinol at concentrations ranging from 1.25 to 25 μM or 6.25 to 200 μM, respectively. The conductance of channels, determined from the slope of the current-voltage relationship, was 33 pS whether the channels were activated by ACh alone or by ACh in combination with an analog. Exposure of endplate membranes to the analogs in the patch pipette produced a marked blocking effect on the receptor ion channel. The channel activity observed in the presence of micromolar concentrations of either *N*-methylanatoxinol isomer consisted of bursts of unitary openings divided by flickers. As shown in Fig. 4 for the *S*-isomer, these flickers occurred more frequently at higher concentrations.

The durations of individual open events were distributed according to a single exponential (Fig. 4) with mean open channel durations dependent upon holding potential and, therefore, also channel amplitude. Both analogs shortened channel open time at high concentrations (Fig. 5). It is possible that the open time at 25 μM *S*-isomer also includes some openings due to its agonist effects.

Quantitative evaluation by multiple regression verified that the alterations created by the *S*-isomer on open channel duration could be modeled well according to a voltage- and concentration-dependent rate of channel blockade. The durations of channel openings decreased at hyperpolarized potentials and in increasing concentrations of the *S*-isomer of *N*-methylanatoxinol, as the rate of blocking (k_3) made increasingly greater contributions to the shortening of mean channel open time (Fig. 5). In the case of the *R*-isomer, the relationship of mean channel open time to concentration was less clear. But, even so, the mean channel open time became progressively shorter from 6.25 to 200 μM. The voltage dependence of k_3 for the *R*-isomer was determined to be insignificant.

When only ACh is present in the pipet, bursts have a low frequency of concentration-independent flickers. These comprise a minor component of the closed duration histograms and the mean durations are voltage independent (11). The fact that two distinct components of closed durations were observed when analogs were added made it possible to associate the shorter population with the more frequent occurrence of channel blockade as analog concentration was increased. The shorter closed times were fitted with single exponentials to

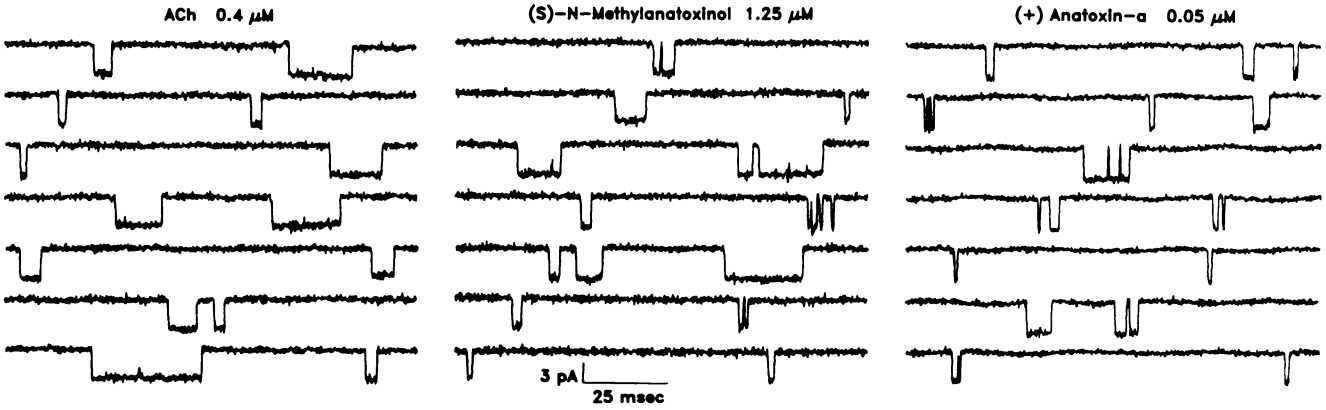

Fig. 2. Single channel currents activated by ACh, (+)-anatoxin-a, and (*S*)-*N*-methylanatoxinol. This figure was purposely designed to show approximately two bursts per trace on a time scale that facilitates comparison of burst characteristics. No indication of potency for channel activation is implied by the frequencies shown. The agonist potencies of ACh and (+)-anatoxin-a are reflected in the low concentrations that are typically used to elicit channel activation. Concentrations of (*S*)-*N*-methylanatoxinol from 1.25 to 125 μM always produced low activation frequencies.

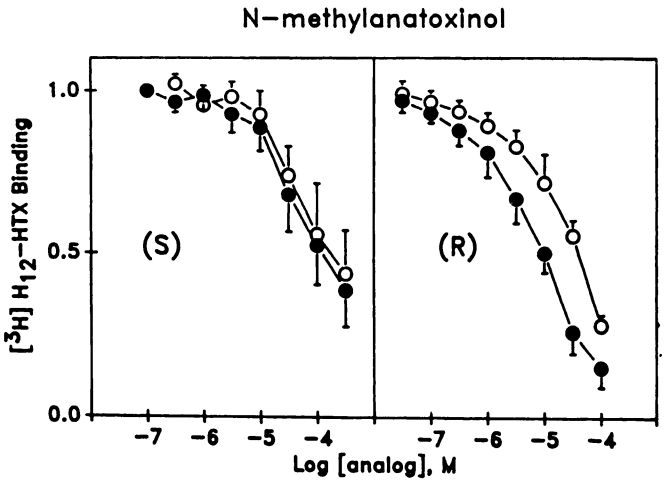

Fig. 3. Influence of *N*-methylanatoxinols on [^{3}H]H_{12}-HTX binding to ion channel sites in the AChR complex. The binding of 2 nM [^{3}H]H_{12}-HTX was measured in the presence of the indicated concentrations of (*S*)- and (*R*)-*N*-methylanatoxinol. Binding was measured in the presence (●) and absence (○) of 1 μM carbamylcholine and is expressed as a fraction of the specific binding measured in the absence of toxins. Each *point* and *bar* represent the mean and standard deviation from three experiments.

TABLE 1

Interactions of *N*-methylanatoxinols with high affinity ion channel sites

For K_i, the errors are expressed as the mean ± standard deviation for three experiments. Values for K_d were calculated for 0 pA (or mV) using parameters in Table 2.

	[^{3}H]H_{12}-HTX K_i		Single Channel, $K_d = k_{-3}/k_3$
	Control	*Carbamylcholine (1 μM)*	
	μM		
(*R*)-*N*-Methylanatoxinol	39 ± 5	8.5 ± 2.1[a]	50
(*S*)-*N*-Methylanatoxinol	170 ± 42	117 ± 56	550
Ratio K_S/K_R	3.9	14	11

[a] Significantly higher affinity than in the absence of carbamylcholine ($p < 0.01$; Student's *t* test).

determine the time constants for unblocking, $\tau_{closed} = 1/k_{-3}$. The τ_{closed} values of the *S*-isomer (2.5 to 25 μM) were independent of drug concentration (Fig. 6). The unblocking time constant for the *S*-isomer was voltage dependent, with greater stability of blockade occurring at more hyperpolarized potentials (Table 2). The rate of recovery from blockade by the *S*-isomer was 1.5 msec^{-1} at an equivalence of −100 mV. In the case of the *R*-isomer, channel closures were longer and k_{-3} was, therefore, somewhat smaller. In this case, no voltage dependence was evident (Fig. 6).

Calculation of affinity constants from the binding and dissociation kinetics measured using the single channel activity (Figs. 5 and 6) suggest that the k_D (at 0 mV) is approximately 10-fold greater for the *S*-isomer than for the *R*-isomer (Table 1). Although the absolute values are greater than those observed to inhibit H_{12}-HTX binding in the presence of carbamylcholine, their ratio corroborates the ratio of their K_i values.

The sequential model predicts conservation of the total open time per burst. In the present cases, despite an increase in the number of openings per burst with increased concentrations, the total open time per burst was decreased (not shown). The burst durations were only decreased to a small extent, compared with the decrease in open channel duration (Fig. 5). The

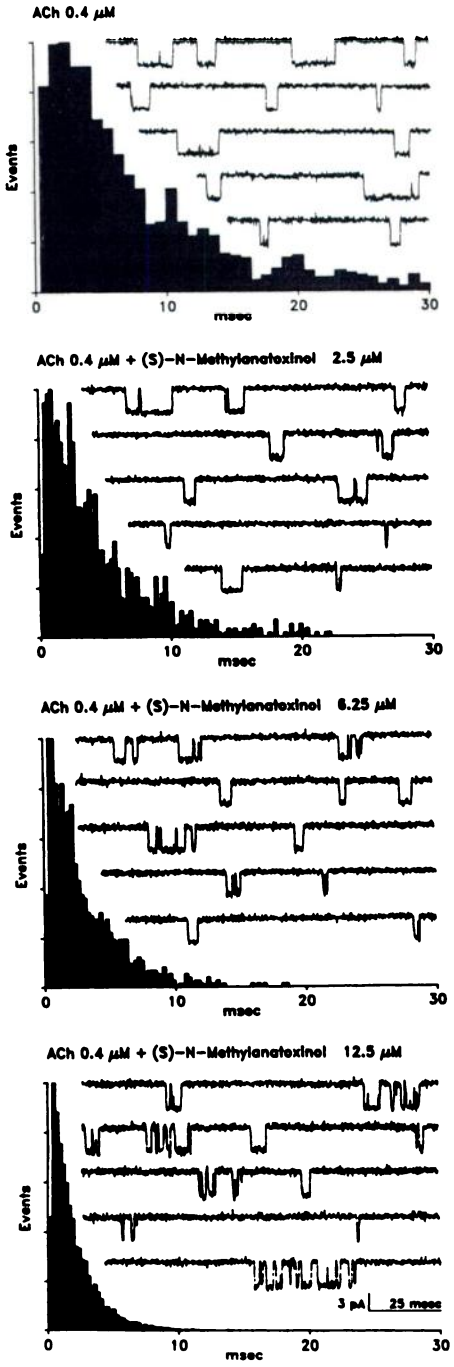

Fig. 4. Concentration-dependent effect of (*S*)-*N*-methylanatoxinol on open times of single channel currents. In the presence of analog, the channels were activated in bursts that were composed of many transitions between open and short blocked states. The channel open times were distributed according to a single exponential function in all cases. Increasing concentrations of anatoxin analog produced successively shorter mean channel durations: control at 3.7 pA, 7.0 msec (n = 1249); 2.5 μM at 3.6 pA, 4.2 msec (n = 1083); 6.2 μM at 3.4 pA, 2.8 msec (n = 939); 12.5 μM at 3.7 pA, 1.7 msec (n = 9876), where n is the total number of open events recorded to generate each histogram.

observed number of openings per burst was on the order of one half of the expected number, based on the data for the blocking rate and the unblocking rate for both drugs (not shown). This may be partly artifactual, based on definition of burst by a minimum interburst interval. For any selected minimum inter-

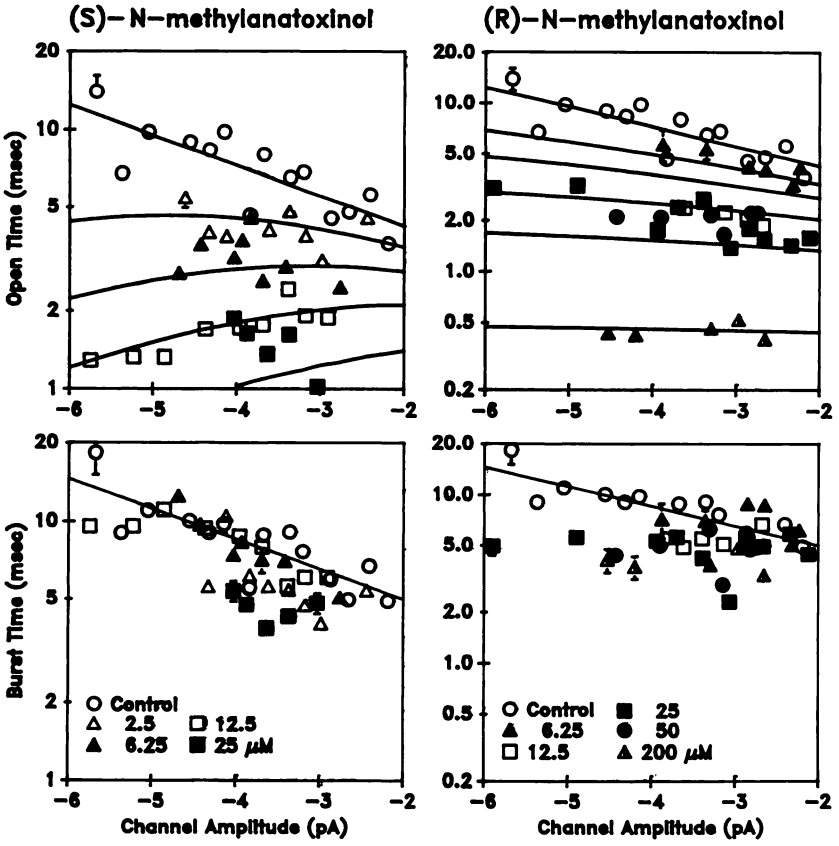

Fig. 5. Voltage-dependence of the mean channel open and burst times. *Upper left*, the mean open times induced by ACh (0.4 μM) alone (control) and in the presence of 2.5 to 25 μM (*S*)-*N*-methylanatoxinol were voltage dependent. The mean open time was prolonged by an increased amplitude in the control condition but was decreased by an increased amplitude in the presence of the *S*-analog. The ion channel-blocking parameters refined by multiple regression of mean open time versus channel amplitude and drug concentration (using data up to 12.5 μM) are listed in Table 2 and the calculated values are shown here as *continuous lines*; *progressively lower lines* are present for each concentration at which observed data are present. The coefficient of multiple determination was 0.909. *Upper right*, the mean channel open times were also shortened by (*R*)-*N*-methylanatoxinol at concentrations above 12.5 μM. Regressions results were calculated using all concentrations and are shown for all concentrations. The blocking rate, k_3, had no significant voltage dependence for the *R*-isomer; see Table 2. The coefficient of multiple determination was 0.868. *Lower left and right*, the burst durations, which are separated from each other by closures greater than 8 msec, were decreased at 25 μM or higher concentrations of either isomer. Standard errors were calculated empirically as mean/$\sqrt{n}$; thus, the few *error bars* that were larger than the *symbols* reflect the large number of channels recorded for each sample.

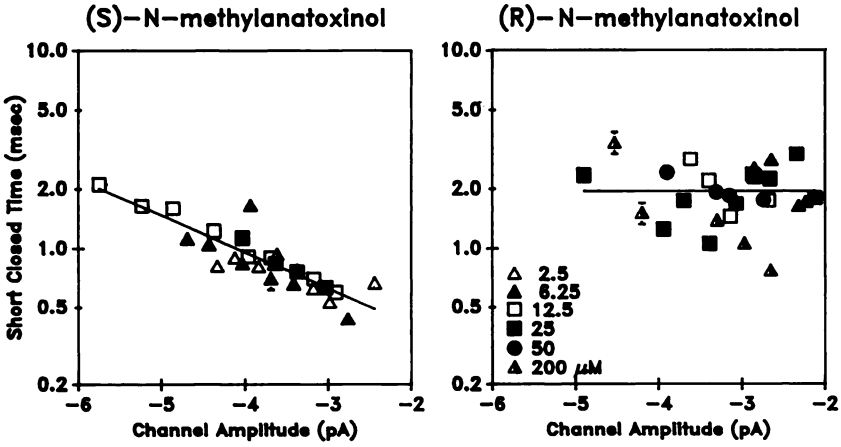

Fig. 6. Voltage dependence of short channel closed times. The mean duration of short closed times ($1/k_{-3}$) showed a clear voltage dependence. From 2.5 to 25 μM *S*-analog, there was no concentration dependence in channel closed times. The slope of the best fit line using data at all concentrations of the analog ($r = 0.879$) indicated an *e*-fold change of closed durations for each 2.32 pA, which corresponds to 71 mV ($k_{-3} = 5.79 \times e^{(14.1 \times V)}$ msec^{-1}). The *R*-isomer caused closures whose durations were voltage independent, and the overall mean was 1.94 msec ($k_{-3} = 0.515$ msec^{-1}). The closed durations of those few short closures observed in the presence of ACh alone (not shown) were approximately 0.15 msec and were apparently not sensitive to voltage.

burst interval, occasional errors will occur in the identification of channel open events as distinct bursts when in fact they were part of a single burst and the closed interval was a long blocked duration. Thus, burst durations, total open time per burst, and the number of channel open events per burst will be underestimated.

It was also possible that the sequential model was incomplete. There probably is an alternate mechanism by which blocked channels are able to close with the channel-blocking ligands still bound to their site on the receptor, without passing through the open state (36–38). The present data on burst duration are neither sufficiently uniform nor of great enough magnitude to warrant modification of the sequential model in a quantitative way.

Discussion

Using biochemical and electrophysiological techniques, we have investigated the *S*- and *R*-epimers of *N*-methylanatoxinol for their contracture potency, affinity of binding to the receptor, and ion channel activation at the nicotinic AChR. The structure of the AChR, particularly the α subunits, is well conserved throughout the vertebrate subphylum (39), making the binding to sites on *Torpedo* electroplaque comparable to pharmacological effects on frog muscle.

In contrast to (+)-anatoxin-a, the *S*-isomer was a much weaker agonist, as demonstrated by its poor ability to inhibit the binding of ^{125}I-α-BGT or to open AChR channels. The *R*-isomer was completely ineffective as an agonist. Similar observations have been made for the binding of these isomers to frog

TABLE 2
Results of least squares fitting of coefficients of kinetic parameters

		B	*A*	Potential for e-Fold Change[a]
		$msec^{-1}$	pA^{-1}	*mV*
k_{-2}	ACh	0.410	0.271	111
		$msec^{-1}\ \mu M^{-1}$		
k_3	*S*	0.0105	−0.289	−106
	R	0.0103		
		$msec^{-1}$		
k_{-3}	*S*	5.79	0.427	71
	R	0.515		

[a] For the convenience of comparison with other voltage-dependent blockers, the voltage-dependent term *A* was also expressed as the voltage that produced an e-fold change in τ by utilizing the relationship that, for 33 pS slope conductance, 1 pA corresponds to 30 mV.

muscle[1]; however, concentrations required to induce contracture were higher than those required to inhibit ^{125}I-α-BGT binding. For example, the *S*-isomer decreased α-BGT binding by 10% at 10 μM but was ineffective at inducing contracture at 170 μM. With the example of (+)-anatoxin-a, contracture became measurable using our techniques at a level close to 25% inhibition of α-BGT binding (11). The deviation could involve a threshold level of receptor activation that is necessary to allow sufficient ion flow for transduction to a mechanical response. Furthermore, the lack of correlation between agonist equilibrium dissociation constants and the concentrations required to elicit muscular responses has been associated with the sensitivity of the binding assay to the desensitized receptor, which has a greater affinity for agonists (8, 40).

Chemical modification of the toxin by methylation alone was not expected to reduce agonist activity, inasmuch as the endogenous ligand ACh and many semi-rigid agonists are quaternary amines (2, 3). However, note that recent observations demonstrate that *N*-methyl- and *N,N*-dimethyl anatoxin have weak agonist effects and significant antagonist effects (41).[2] At the other site of modification, the reduction of the ketone moiety to a secondary alcohol weakened the forces for hydrogen bonding to the agonist site of the AChR (4, 20). The elimination of the conjugated enone system permitted rotation and, hence, variation in the nitrogen-hydrogen bond separation and loss of planarity present in ester agonists (5) and (+)-anatoxin-a (22). Further details regarding molecular conformation and agonist potency of anatoxin derivatives must be addressed elsewhere.

The important new aspect of these isomers was that they produced a concentration-dependent blockade of the AChR. It is a particular problem in the evaluation of nicotinic agonists that many agonists and agonist-like compounds are also noncompetitive antagonists of the AChR at micromolar concentrations (20, 42–44). Anatoxin-a at concentrations up to 0.2 μM did not produce blockade of the AChR (1, 11). For the *N*-methylanatoxinols, the inhibition of H_{12}HTX binding and flickering in the single channel currents were the more sensitive indicators of receptor antagonism, whereas the twitch response was slightly affected only by the *R*-isomer.

The rates of ion channel blocking and unblocking were voltage dependent for the *S*-isomer, but not so for the *R*-isomer. These voltage dependencies (Table 2) indicated that the blockade induced by the *S*-isomer was stabilized at hyperpolarized potentials. What could account for the voltage sensitivity of the *S*-isomer, i.e., more rapid binding at hyperpolarized membrane potentials and more rapid dissociation at depolarized membrane potentials, in contrast to the lack of voltage sensitivity of the *R*-isomer? Similar voltage dependence has been noted for other charged blocking drugs (31, 42, 45, 46). In contrast, the lack of voltage dependence seen with the *R*-isomer has been noted with nonpolar compounds (45, 47).

Polar charged and nonpolar drugs may have access to the binding site via hydrophilic and hydrophobic pathways, respectively (48). Relative hydrophobicity within a series of analogs is correlated with greater antagonist potency (24, 49–52). Access of blockers to their binding site was facilitated by nicotinic agonists, as revealed by a faster rate of association of [^{3}H]H_{12}HTX with the ion channel site (26, 52–54). In these experiments, the *R*-isomer was more potent in causing inhibition of [^{3}H]H_{12}HTX binding than the *S*-isomer, in the absence of carbamylcholine. In the presence of carbamylcholine, the affinity of the *R*-isomer of *N*-methylanatoxinol for the ion channel sites became even greater. The high affinity (hydrophobic) blockers within series of chemically related channel blockers were particularly sensitive to agonist, but the binding of very weak channel blockers is frequently insensitive to receptor agonists. This may explain why the affinity of the *R*-isomer, but not the S-isomer, is increased in the presence of carbachol.

Thus, one may be led to the presumption that differences in polarity of the isomers could account for the differences in voltage sensitivity and agonist sensitivity. However, differences in polarity of the isomers were *not* noted using thin layer chromatography. Although there are only small structural differences between the two isomers, the binding-dissociation properties of the two isomers in the present study suggest that dual stereochemical parameters were active. The *S*-isomer could achieve a greater rate of binding via long range coulombic forces of attraction to the receptor. For the *R*-isomer, short range van der Waals forces may explain both slower binding and slower dissociation, if it is presumed to fit the receptor more ideally. Thus, the differences in pharmacological properties might arise from stereospecific or stereospecifically induced differences in drug-receptor interactions. Note that stereospecificity for ion channel blockade has not previously been found (47).

The reasons for the systematic differences observed between the biochemical and electrophysiological interaction constants could be attributed to the sensitivity of the equilibration measurements to ionic composition, exposure to receptor ligands, or perhaps even to the desensitized state of the receptor. Additionally, the different species and tissues used or the unknown transmembrane potential in the membrane preparation could account for even more discrepancy. Although the potential difference across the membranes used in binding studies has not been measured (26), it is possible to conjecture using the kinetic and equilibrium data for the *S*-isomer. The data suggest that the receptor in the homogenized tissue responds in a manner similar to that of the receptor in isolated muscle fibers held at a hyperpolarized potential. Many other conditions may contribute and, therefore, a number of issues remain to be addressed in correlating binding and kinetic data.

During the physiologically synchronized activity of neuromuscular transmission, the channel-blocking properties of these analogs could alter the decay of endplate currents. A greater depression of the endplate potential by the *R*-isomer

[1] S. Wonnacott and E. X. Albuquerque, unpublished observations.
[2] P. Kofuji and K. L. Swanson, unpublished observations.

than the *S*-isomer is predicted, due to the lack of voltage dependence of the *R*-isomer. During normal synaptic depolarization and action potential generation, blockade by the *S*-isomer would be reversed; hence, it is a weaker blocker than the *R*-isomer. This is confirmed by the lower potency of the *S*-isomer for the antagonism of H_{12}-HTX binding and muscle twitch.

Beyond the purely biophysical issues that this study has addressed, we can consider the possible applications of drugs that on first test did not elicit contracture and only weakly antagonized muscle twitch. Compounds having reversible blocking properties like those described here might effectively compete with the action of other channel blockers, particularly those that have slow reversal kinetics, such as phencyclidine (49) or cocaine (38). The concept of antagonist reversal by use of other antagonists with rapid kinetics has been noted previously for competitive antagonists (55). Therapeutic agents specific for reversal of nicotinic ion channel blockade are not currently well known. In the case of oximes, the reversible channel-blocking actions contributed significantly to antagonism of organophosphate poisoning (46). Low intrinsic pharmacological efficacy or potency should be advantageous in an antidotal or prophylactic regimen against nicotinic blockade.

Acknowledgments

We thank Ms. Mabel A. Zelle and Mrs. Barbara Marrow for their expert computer and technical assistance. F. J. S. thanks the Spanish Ministry of Education.

References

1. Spivak, C. E., B. Witkop, and E. X. Albuquerque. Anatoxin-a: a novel, potent agonist at the nicotinic receptor. *Mol. Pharmacol.* **18**:384–394 (1980).
2. Spivak, C. E., J. Waters, B. Witkop, and E. X. Albuquerque. Potencies and channel properties induced by semirigid agonists at frog nicotinic acetylcholine receptors. *Mol. Pharmacol.* **23**:337–343 (1983).
3. Spivak, C. E., and E. X. Albuquerque. Dynamic properties of the nicotinic acetylcholine receptor ionic channel complex: activation and blockade, in *Progress in Cholinergic Biology: Model Cholinergic Synapses* (I. Hanin and A. M. Goldberg, eds.). Raven Press, New York, 323–357 (1982).
4. Beers, W. H., and E. Reich. Structure and activity of acetylcholine. *Nature (Lond.)* **288**:917–922 (1970).
5. Chothia, C., and P. Pauling. The conformation of cholinergic molecules at nicotinic nerve receptors. *Proc. Natl. Acad. Sci. USA* **65**:477–482 (1970).
6. Langenbuch-Cachat, J., C. Bon, C. Mulle, M. Goeldner, C. Hirth, and J.-P. Changeux. Photoaffinity labeling of the acetylcholine binding sites on the nicotinic receptor by an aryldiazonium derivative. *Biochemistry* **27**:2337–2345 (1988).
7. Dennis, M., J. Giraudat, F. Hibert, M. Goeldner, C. Hirth, J.-Y. Chang, C. Lazure, M. Chrétien, and J.-P. Changeux. Amino acids of the *Torpedo marmorata* acetylcholine receptor α subunit labeled by a photoaffinity ligand for the acetylcholine binding site. *Biochemistry* **27**:2346–2357 (1988).
8. Prinz, H., and A. Maelicke. Interaction of cholinergic ligands with purified acetylcholine receptor proteins. I. Equilibrium binding studies. *J. Biol. Chem.* **258**:10263–10271 (1983).
9. Prinz, H., and A. Maelicke. Interaction of cholinergic ligands with purified acetylcholine receptor protein. II. Kinetic studies. *J. Biol. Chem.* **258**:10273–10282 (1983).
10. Carmichael, W. W., D. F. Biggs, and P. R. Gorham. Toxicology and pharmacological action of *Anabaena flos*-aquae toxin. *Science (Wash., D. C.)* **187**:542–544 (1975).
11. Swanson, K. L., C. N. Allen, R. S. Aronstam, H. Rapoport, and E. X. Albuquerque. Molecular mechanisms of the potent and stereospecific nicotinic receptor agonist (+)-anatoxin-a. *Mol. Pharmacol.* **29**:250–257 (1986).
12. Aronstam, R. S., and B. Witkop. Anatoxin-a interaction with cholinergic synaptic molecules. *Proc. Natl. Acad. Sci. USA* **78**:4639–4643 (1981).
13. Macallan, D. R. E., G. G. Lunt, S. Wonnacott, K. L. Swanson, H. Rapoport, and E. X. Albuquerque. Methyllycaconitine and (+)-anatoxin-a differentiate between nicotinic receptors in vertebrate and invertebrate nervous systems. *FEBS Lett.* **226**:357–363 (1987).
14. Zhang, X., P. Stjernlöf, A. Adem, and A. Nordberg. Anatoxin-a, a potent ligand for nicotinic cholinergic receptors in rat brain. *Eur. J. Pharmacol.* **135**:457–458 (1987).
15. Aracava, Y., S. S. Deshpande, K. L. Swanson, H. Rapoport, S. Wonnacott, G. Lunt, and E. X. Albuquerque. Nicotinic acetylcholine receptors in cultured neurons from the hippocampus and brain stem of the rat characterized by single channel recording. *FEBS Lett.* **222**:63–70 (1987).
16. Whitehouse, P. J., and K. J. Kellar. Nicotinic and muscarinic cholinergic receptors in Alzheimer's disease and related disorders. *J. Neural Trans. Suppl.* **24**:175–182 (1987).
17. Nordberg, A., P. Nyberg, R. Adolfsson, and B. Winblad. Cholinergic topography in Alzheimer brains: a comparison with changes in the monoaminergic profile. *J. Neural Trans.* **69**:19–32 (1987).
18. Perry, E. K., R. H. Perry, C. J. Smith, D. J. Dick, J. M. Candy, J. A. Edwardson, A. Fairbairn, and G. Blessed. Nicotinic receptor abnormalities in Alzheimer's and Parkinson's Diseases. *J. Neurol. Neurosurg. Psych.* **50**:806–809 (1987).
19. Aracava, Y., K. L. Swanson, R. Rozental, and E. X. Albuquerque. Structure-activity relationships of (+)-anatoxin-a derivatives and enantiomers of nicotine on the peripheral and central nicotinic acetylcholine receptor subtypes, in *Molecular Basis of Drug and Pesticide Action* (G. G. Lunt, ed.) Elsevier Publ., Cambridge, U. K., in press (1988).
20. Waksman, G., J.-P. Changeux, and B. P. Roques. Structural requirements for agonist and noncompetitive blocking action of acylcholine derivatives on *Electrophorus electricus* electroplaque. *Mol. Pharmacol.* **18**:20–27 (1980).
21. Rozental, R., Y. Aracava, K. L. Swanson, and E. X. Albuquerque. Nicotine: interactions of its stereoisomers with the nicotinic acetylcholine receptor. *Soc. Neurosci. Abstr.* **13**:709 (1987).
22. Koskinen, A. M. P., and H. Rapoport. Synthetic and conformational studies on anatoxin-a: a potent acetylcholine agonist. *J. Med. Chem.* **28**:1301–1309 (1985).
23. Lemke, T. *Review of Organic Functional Groups: Introduction to Medicinal Chemistry.* Lea and Febiger, Philadelphia (1988).
24. Aronstam, R. S., C. T. King, E. X. Albuquerque, J. W. Daly, and D. M. Feigl. Binding of [^{3}H]perhydrohistrinonicotoxin and [^{3}H]phencyclidine to the nicotinic receptor-ion channel complex of *Torpedo* electroplax: inhibition by histrionicotoxins and derivatives. *Biochem. Pharmacol.* **34**:3037–3047 (1985).
25. Tsai, M.-C., N. A. Mansour, A. T. Eldefrawi, M. E. Eldefrawi, and E. X. Albuquerque. Mechanism of action of amantadine on neuromuscular transmission. *Mol. Pharmacol.* **14**:787–803 (1978).
26. Aronstam, R. S., A. T. Eldefrawi, I. N. Pessah, J. W. Daly, E. X. Albuquerque, and M. E. Eldefrawi. Regulation of [^{3}H]perhydrohistrionicotoxin binding to *Torpedo ocellata* electroplax by effectors of the acetylcholine receptor. *J. Biol. Chem.* **22**:3128–3136 (1981).
27. Allen, C. N., A. Akaike, and E. X. Albuquerque. The frog interosseal muscle fiber as a new model for patch clamp studies of chemosensitive and voltage-sensitive ion channels: actions of acetylcholine and batrachotoxin. *J. Physiol. (Paris)* **79**:338–343 (1984).
28. Aracava, Y., S. R. Ikeda, J. W. Daly, N. Brookes, and E. X. Albuquerque. Interactions of bupivacaine with ionic channels of the nicotinic receptor: analysis of single channel currents. *Mol. Pharmacol.* **26**:304–313 (1984).
29. Colquhoun, D., and F. J. Sigworth. Fitting and statistical analysis of single-channel records, in *Single-Channel Recording* (B. Sakmann and E. Neher, eds.). Plenum Press, New York, 191–263 (1983).
30. Steinbach, A. B. A kinetic model for the action of xylocaine on receptors for acetylcholine. *J. Gen. Physiol.* **52**:162–180 (1968).
31. Adler, M., E. X. Albuquerque, and F. J. Lebeda. Kinetic analysis of end plate currents altered by atropine and scopolamine. *Mol. Pharmacol.* **14**:514–529 (1978).
32. Magleby, K. L., and C. F. Stevens. The effect of voltage on the time course of end-plate currents. *J. Physiol. (Lond.)* **223**:151–171 (1972).
33. Neher, E., and J. H. Steinbach. Local anaesthetics transiently block currents through single acetylcholine-receptor channels. *J. Physiol. (Lond.)* **277**:153–176 (1978).
34. Caceci, M. S., and W. P. Cacheris. Fitting curves to data: the simplex algorithm is the answer. *BYTE* **9**:340–362 (1984).
35. Walpole, R. E., and R. H. Myers. *Probability and Statistics for Engineers and Scientists*, 3rd Ed. Macmillan, New York (1985).
36. Adams, P. R. Voltage jump analysis of procaine action at frog end-plate. *J. Physiol. (Lond.)* **268**:291–318 (1977).
37. Neher, E. The charge carried by single-channel currents of rat cultured muscle cells in the presence of local anaesthetics. *J. Physiol. (Lond.)* **339**:663–678 (1983).
38. Swanson, K. L., and E. X. Albuquerque. Nicotinic ion channel blockade by cocaine: the primary mechanism of synaptic action. *J. Pharmacol. Exp. Ther.* **243**:1202–1210 (1987).
39. Changeux, J.-P., A. Devillers-Thiéry, and P. Chemouilli. Acetylcholine receptor: an allosteric protein. *Science (Wash. D. C.)* **225**:1335–1345 (1984).
40. Colquhoun, D., and H. P. Rang. Effects of inhibitors on the binding of iodinated α-bungarotoxin to acetylcholine receptors in rat muscle. *Mol. Pharmacol.* **12**:519–535 (1976).
41. Costa, A. C. S., Y. Aracava, H. Rapoport, and E. X. Albuquerque. *N,N*-dimethylanatoxin: an electrophysiological analysis. *Neurosci. Abstr.* **14**:1327 (1988).
42. Adams, P. R., and B. Sakmann. Decamethonium both opens and blocks endplate channels. *Proc. Natl. Acad. Sci. USA* **75**:2994–2998 (1978).
43. Lambrecht, G. Struktur- und konformations-wirkungs-Beziehungen heterozyklischer Acetylcholin-Analoga. 12. Mittelung: Synthese und cholinerge Eigenschaften stereoisomerer 3-Acetoxythiacyclohexane. *Arzneim. Forsch.* **31**:634–640 (1981).

44. Milne, R. J., and J. H. Byrne. Effects of hexamethonium and decamethonium on end-plate current parameters. *Mol. Pharmacol.* **19**:276–281 (1981).
45. Pennefather, P., and D. M. J. Quastel. Actions of anesthetics on the function of nicotinic acetylcholine receptors, in *Molecular Mechanisms of Anesthesia Progress in Anesthesiology* (B. F. Fink, ed.), Vol. 2. Raven Press, New York (1980).
46. Alkondon, M., K. S. Rao, and E. X. Albuquerque. Acetylcholinesterase reactivators modify the functional properties of the nicotinic acetylcholine receptor ion channel. *J. Pharmacol. Exp. Ther.* **245**:543–556 (1988).
47. Henderson, F., C. Prior, J. Dempster, and I. G. Marshall. The effects of chloramphenicol isomers on the motor end-plate nicotinic receptor-ion channel complex. *Mol. Pharmacol.* **29**:52–64 (1986).
48. Blanton, M., E. Mccardy, T. Gallaher, and H. H. Wang. Noncompetitive inhibitors reach their binding site in the acetylcholine receptor by two different paths. *Mol. Pharmacol.* **33**:634–642 (1988).
49. Aguayo, L., and E. X. Albuquerque. Effects of phencyclidine and its analogs on the end-plate current of the neuromuscular junction. *J. Pharmacol. Exp. Ther.* **239**:15–24 (1986).
50. Aronstam, R. S., J. W. Daly, T. F. Spande, T. K. Narayanan, and E. X. Albuquerque. Interaction of gephyrotoxin and indolizidine alkaloids with the nicotinic acetylcholine receptor-ion channel complex of *Torpedo* electroplax. *Neurochem. Res.* **11**:1227–1240 (1986).
51. Aronstam, R. S., M. W. Edward, J. W. Daly, and E. X. Albuquerque. Interactions of piperidine derivatives with the nicotinic cholinergic receptor complex from *Torpedo* electric organ. *Neurochem. Res.* **13**:171–176 (1988).
52. Albuquerque, E. X., J. W. Daly, and J. E. Warnick. Macromolecular sites for specific neurotoxins and drugs on chemosensitive synapses and electrical excitation in biological membranes, in *Ion Channels* (T. Narahashi, ed.). Plenum Press, New York, 95–162 (1988).
53. Oswald, R. E., T. Heidmann, and J.-P.Changeux. Multiple affinity states for noncompetitive blockers revealed by [^{3}H]phencyclidine binding to acetylcholine receptor rich membranes from *Torpedo marmorata*. *Biochemistry* **22**:3128–3136 (1983).
54. Heidmann, T., R. E. Oswald, and J.-P. Changeux. Multiple sites of action for noncompetitive blockers on acetylcholine receptor rich membrane fragments from *Torpedo marmorata*. *Biochemistry* **22**:3112–3127 (1983).
55. Ginsborg, B. L., and R. P. Stephenson. On the simultaneous action of two competitive antagonists. *Br. J. Pharmacol.* **51**:287–300 (1974).

Send reprint requests to: Dr. E. X. Albuquerque, Department of Pharmacology and Experimental Therapeutics, University of Maryland School of Medicine, Baltimore, MD 21201.